ARTICLE

Detection of OH Radical in the Photodissociation of p-Aminobenzoic Acid at 266 nm†

Can-hua Zhou, Shi-bo Cheng, Hong-ming Yin*, Guo-zhong He

State Key Laboratory of Molecular Reaction Dynamics, Dalian Institute of Chemical Physics, Chinese Academy of Sciences, Dalian 116023, China

(Dated: Accepted on November 24, 2009)

Photodissociation of p-aminobenzoic acid at 266 nm was investigated by probing the nascent OH photoproduct employing the laser-induced fluorescence technique. It was found that the nascent OH radical was vibrationally cold and its rotational state distribution conformed to be a Boltzmann behavior, characterized by a rotational temperature of 1040±110 K. The rotational energy of OH was determined to be 8.78±0.84 kJ/mol. Between the two spin-orbit states of OH, $^2\Pi_{3/2}$ and $^2\Pi_{1/2}$, the former was found to be preferentially populated. The distribution of the $\Pi(A')$ state for the Λ-doublet was dominant. Finally, a probable mechanism for the formation of OH produced from the photodissociation of p-aminobenzoic acid is discussed.

Key words: Photodissociation, OH radical, p-aminobenzoic acid, Laser-induced fluorescence technique

I. INTRODUCTION

Photodissociation of carboxylic acids has been investigated extensively [1−9] because it generates the OH radical, which is the most important chemical cleaning agent of the atmosphere [10] and the main oxidizing agent in the troposphere, where it reacts with most trace pollutant gases [11]. Kim *et al.* and Naik *et al.* have studied the photolysis of acetic acid at 193 nm, respectively [1,2]. They found that the dissociation takes place indirectly along the triplet surface via curve crossing with the reverse barrier in the exit channel. Kumar *et al.* have studied the photodissociation of saturated [3,4] and unsaturated [5,6] carboxylic acids at 193 and 248 nm. They observed an appreciable amount of energy being channeled into the relative translation of OH and its co-fragment. Recently, our group has investigated the photodissociation of benzoic acid [7,8] and *o*-nitrobenzoic acid [9] at different photolysis wavelengths. It was revealed that these acids undergo dissociation to produce OH radical from the excited state with an exit barrier.

Similar to other carboxylic acids, p-aminobenzoic acid (PABA), which is an important conjugated compound of biological, medicinal, and industrial interest, and widely used as active ingredient in commercial sunscreens and dietary supplements [12,13], has attracted much attention due to both its biological importance and its chemical properties. Most of the works related to PABA are mainly focused on its thermodynamics and spectroscopic properties [14−21]. Using laser desorption, the resonantly enhanced multiphoton ionization (REMPI) spectra of bare PABA and its complexes with argon, methanol and water have been recorded [14]. Spectroscopic properties of the PABA complexes with water have been characterized by two-color REMPI spectroscopy [15]. Supersonically cooled PABA has also been studied using one-color REMPI and two-color zero kinetic energy (ZEKE) photoelectron spectroscopy [16]. Macroscopic and microscopic thermodynamic quantities for proton ionization from protonated PABA in aqueous solutions at temperatures from 298.15 K to 393.15 K have been determined by a combination of NMR, potentiometric, and calorimetric methods [17]. The permanent dipole moment of PABA has been measured [18,19] and calculated at various theoretical levels [20]. PABA has also been investigated by density functional theory, Møller-Plesset perturbation theory and composite *ab initio* methods to determine reliable thermochemical data as well as vertical and adiabatic ionization energies for this molecule [21]. However, the photochemical study of PABA in the gas phase received very scarce attention. Therefore, it is worthwhile to investigate the photodissociation of PABA to generate the nascent OH radical, which is also a continuation and extension of our previous studies on photolysis of benzoic acid [7,8].

In this work, we have detected the nascent OH fragment by employing the laser-induced fluorescence (LIF) technique after photolysis of the excited PABA

†Part of the special issue for "the Chinese Chemical Society's 11th National Chemical Dynamics Symposium".

*Author to whom correspondence should be addressed. E-mail: hm_yin@dicp.ac.cn

at 266 nm under collision-free conditions. By analyzing the LIF spectrum, the internal state distribution of the nascent OH radical was obtained. According to the experimental results, a probable mechanism of PABA photodissociation leading to OH formation is discussed.

II. EXPERIMENTS

The experimental setup used in the present work has been described in detail elsewhere [22−24]. Here, only a brief description about the apparatus is given. The second-harmonic output (532 nm) of a seeded Nd:YAG laser (Spectra-Physics, GCR-170) was converted into 266 nm by a KD*P crystal, which was used as the photolysis laser. Another second-harmonic output (532 nm) of a seeded Nd:YAG laser (Spectra-Physics, PRO-190) was used to pump a dye laser (Coherent, SCANMATE-PRO), which generated the wavelength-tunable laser pulses. The dye laser was operated with DCM dye, of which the corresponding fundamental wavelength tuning range is 600−640 nm. The output of the dye laser was checked by a laser wavelength meter (Coherent) and then introduced into a harmonic generator (Coherent, Scanmate-SHG) to produce the frequency-doubled UV laser pulses in the 300−320 nm region, which were used as the probe laser. The pulse energies used in the experiments were about 1.5 and 0.02 mJ for the photolysis and probe laser beams, respectively. Both the photolysis and probe beams were collinearly counter propagated through the center of the photolysis cell. The probe laser was delayed 15 ns with respect to the photolysis laser, which was controlled by a generator (SRS, DG535). This delay was sufficient to separate the two laser pulses, and was short enough to avoid collision effects under the pressure (typically 26.6 Pa) during the experiments.

The OH fragment was probed by exciting the $A^2\Sigma^+(v'=0)\leftarrow X^2\Pi(v''=0)$ transition of OH and monitoring the subsequent $A\rightarrow X$ fluorescence. The fluorescence of the OH fragment was collected by a photomultiplier tube (PMT, Hamamatsu CR161). A suitable band filter (λ_{center}=310 nm, full width at half maximum is 15 nm) was placed between the collecting lens and the PMT to cut off scattering from the photolysis laser and the probe laser. The signal was averaged by a boxcar (SRS, SR250), A/D converted by a homemade interface, and stored into a personal computer. In the experiments, saturation effect was avoided by keeping the laser beam energies low enough to observe a linear behavior of the LIF intensity with respect to the variations of the powers of each laser and the sample pressure of the photolysis cell.

PABA (≥99.5%) was purchased from Shengyang Lianbang Chemicals Reagents Company and used without further purification. During the experiments, the sample was heated to 470 K, helium carrier gas was bubbled through the sample, and the gas mixture was continuously expanded into the center of the photolysis cell.

III. RESULTS AND DISCUSSION

The LIF spectrum of the OH fragment from PABA photolysis at 266 nm was recorded by scanning the OH $A^2\Sigma^+(v'=0)\leftarrow X^2\Pi(v''=0)$ transition in the 306−315 nm range. In our experiments, the nascent OH radical was formed in the vibrational ground state. Figure 1(a) shows the experimental LIF excitation spectrum of the (0,0) band of the nascent OH formed upon photolysis at 266 nm. In order to precisely assign the J'' levels of OH populated in the dissociation process, it is necessary to compare the experimental spectrum with the simulated one calculated from the known spectroscopic constants [25]. The rotational state population $N(J'',\ v'')$ in the ground electronic state could be obtained from the intensities of the observed LIF rotational lines. The relationship between the intensities of the fluorescence signal (I_{F}) and the rovibrational state populations $N(J'',\ v'')$ is expressed by

$$I_{\text{F}} \propto \frac{N(J'', v'')q_{v'v''}S_{J'J''}f(\nu,\nu_0)}{2J''+1} \tag{1}$$

where $q_{v'v''}$ is the known Franck-Condon factor for the OH $A\rightarrow X$ transition [26], $S_{J'J''}$ is the known Honl-London factor for the OH $A\rightarrow X$ one-photon rotational transitions [27], and $f(\nu,\ \nu_0)=\rho(\nu_0)\exp[-\alpha(\nu-\nu_0)^2]$ is the laser intensity function. The simulated spectrum of the OH (0,0) band corresponding to the photolysis wavelength of 266 nm is plotted in Fig.1(b).

The OH transitions are labeled following Hund's case (a). The P, Q, or R branches are for cases in which

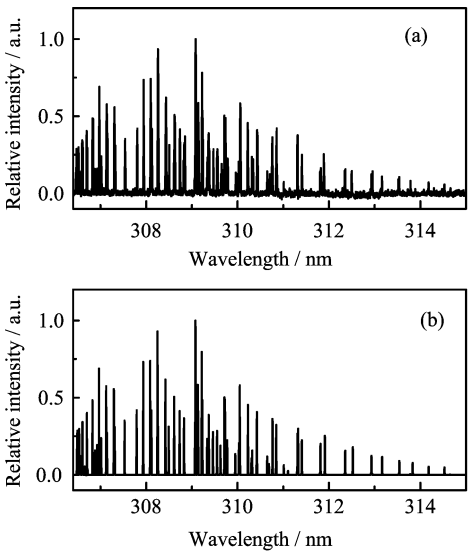

FIG. 1 The LIF excited spectra of the nascent OH ($A^2\Sigma^+(v'=0)\leftarrow X^2\Pi(v''=0)$) fragment from the photodissociation of PABA at 266 nm: (a) experiment and (b) simulation.

DOI:10.1088/1674-0068/22/06/681-685

ΔJ=−1, 0, or 1, and the subscript 1 or 2 represent the different spin-orbit states $^2\Pi_{3/2}$ or $^2\Pi_{1/2}$, respectively. According to the parity selection rule (+↔−), the Q branch only corresponds to the Π(A″) state, while the P and R branches are attributed to the Π(A′) state. Spin-orbit coupling and the Λ-doublet ratios are calculated from the relative population of different rotational states. Detailed analysis of the quantum state distributions of the OH fragment is presented as follows.

A. Rotational state distribution

The OH rotational distribution at 266 nm photolysis of PABA is determined by analyzing of P_1 and P_2 rotational lines, because these lines are mostly free of interference from other lines. In order to compare the measurements of each rotational level, the intensities of the observed LIF rotational lines have been normalized with respect to the pressure in the photolysis cell, the energies of the probe laser, and the photolysis laser. On the basis of the normalized experimental data, the rotational state distribution could be characterized by a Boltzmann temperature from the expression of the Boltzmann population distribution

$$\ln \frac{N(J'')}{2J''+1} = -\frac{\varepsilon(J'')hc}{kT_R} + \text{constant} \qquad (2)$$

A typical Boltzmann plot obtained from 266 nm photodissociation of PABA is shown in Fig.2. The solid line is the best linear fit to the experimental data, and the rotational temperature is about 1040±110 K calculated from the line slope. Additionally, the corresponding rotational energies of the ground state $X^2\Pi(v''=0)$ is calculated to be 8.78±0.84 kJ/mol using $E_v^{\text{rot}}=\sum_{J''} p(J'')\varepsilon(J'')$ including both the two spin-orbit states, where $p(J'')$ is the relative state population and $\varepsilon(J'')$ is the energy of a given rotational state.

In addition, to see whether any OH is produced in the v''=1 level, the OH $A^2\Sigma^+(v'=1)\leftarrow X^2\Pi(v''=1)$ transition was scanned. However, no LIF signal of the OH photofragment ($X^2\Pi$, v''=1) was observed from the photodissociation of PABA at 266 nm, which suggests that the OH fragment is mostly populated in v''=0 in our experiments.

B. Spin-orbit state distribution

Since the electronic spin has a value of 1/2 in the OH radical, the interaction of the electronic spin with the orbital angular momentum splits the $X^2\Pi$ state into two spin orbit components, $^2\Pi_{3/2}$ and $^2\Pi_{1/2}$. Populations of the two spin-orbit states, $^2\Pi_{3/2}$ and $^2\Pi_{1/2}$, can be obtained from the intensities of $P_1(Q_1)$ and $P_2(Q_2)$ lines, respectively. The ratios of the population of the $^2\Pi_{3/2}$ and $^2\Pi_{1/2}$ states are plotted versus the rotational quantum number J'' in Fig.3. As can be seen from the plot, the OH fragment exhibits a preferential population of the $^2\Pi_{3/2}$ state with a relative value of 1.5±0.3. The distinct deviation of the measured spin-orbit ratio from the statistical value could be explained partly based on energy difference between these two states: the $^2\Pi_{1/2}$ state lies higher in energy than the $^2\Pi_{3/2}$ state at the same J''. The preferential population of the $^2\Pi_{3/2}$ state also indicates a coupling between the initially prepared excited singlet state with a nearby triplet state [28−31].

C. Λ-doublet state distribution

The Λ-doublet splitting arises due to the interaction between orbital angular momentum and nuclear rotation, and this interaction is of different magnitude for two Λ-doublet states, Π(A′) and Π(A″). These two states in the OH radical are created by different orientations of the Π lobes with respect to the plane of rotation. In the Π(A′) state, the pπ lobe lies in the

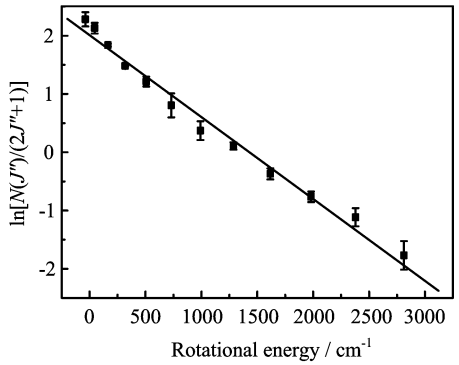

FIG. 2 The Boltzmann plot for the rotational state distributions of the nascent OH fragment generated from the photolysis of PABA at 266 nm. The solid line is the best fit to the data points and represents a rotational temperature of 1040±110 K.

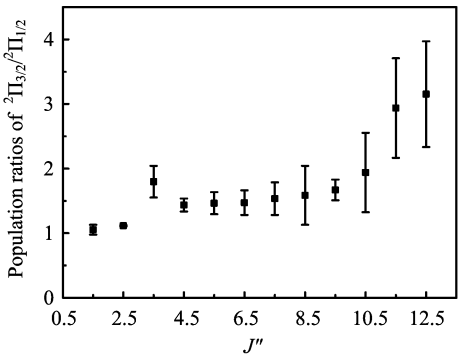

FIG. 3 Ratios of the rotational state distribution of $^2\Pi_{3/2}/^2\Pi_{1/2}$ versus the rotational quantum number J'' of the nascent OH($X^2\Pi$, v''=0) fragment after PABA photolysis at 266 nm. Preferential population of the $^2\Pi_{3/2}$ spin-orbit state of OH is observed.

DOI:10.1088/1674-0068/22/06/681-685

plane of rotation; whereas in the $\Pi(A'')$ state, the $p\pi$ lobe is perpendicular to the plane of rotation. As mentioned earlier, the Q branch is used for detecting the OH fragment in the $\Pi(A'')$ state, whereas the R and P branches are used for that in the $\Pi(A')$ state. Thus, the R/Q (or P/Q) intensity ratios represent the ratios of the Λ-doublet, which give information about the relative population of the OH fragment in the $\Pi(A')$ and $\Pi(A'')$ states [32]. In Fig.4, the Λ-doublet ratios for the $^2\Pi_{3/2}$ state obtained from the P_1/Q_1 ratio are shown with the function of rotational quantum number J''. It can be seen that the states are unequally populated, with a Λ-doublet population ratio $\Pi(A')/\Pi(A'')$ of 1.8±0.3, implying a preferential population of OH in the $\Pi(A')$ state at this photolysis wavelength. This result suggests that the $p\pi$ electronic orbital of the OH radical is predominantly in its plane of rotation.

D. General discussion of mechanism for OH formation

Since the molecular structure of PABA contains the carboxylic group, OH formation should be involved the direct cleavage of the C−OH bond in the carboxylic group. In the present investigation, only 8.78 kJ/mol of the available energy is distributed into OH internal energy, on photolysis of PABA at 266 nm. The low internal energy distribution of OH from PABA photolysis is very similar to that of some other carboxylic acids [5−9], which indicates the presence of a considerable barrier in the OH exit channel. Thus OH is likely formed on an electronically excited potential energy surface, since dissociation from the ground electronic state is essentially barrierless [3−6]. As mentioned above, the preferential population of the $^2\Pi_{3/2}$ state is observed, indicating a coupling between the initially prepared excited singlet state with a nearby triplet state. Hence, the competing dissociation channel of PABA occurred on the triplet electronic excited state seems to be a dominant channel. Furthermore, the relative population of the Λ-doublet of OH provides the exit channel dynamics in the bond cleavage process. The nonstatistical ratio of the Λ-doublet suggests that the transition state for the OH formation channels is slightly nonplanar in nature.

According to the above discussion, it is concluded that on photolysis of PABA at 266 nm, the nascent OH fragment is formed mainly on the electronic excited state via the direct cleavage reaction of the C−OH bond in the carboxylic group with a considerable barrier in the exit channel.

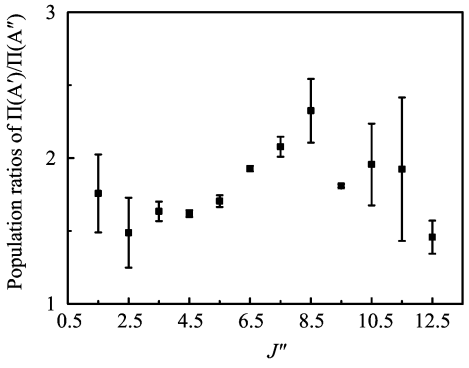

FIG. 4 The relative Λ-doublet population versus the rotational quantum number J'' of the nascent $OH(X^2\Pi, v''=0)$ fragment from the photolysis of PABA at 266 nm. The $\Pi(A')$ state is populated in preference to the $\Pi(A'')$ state.

IV. CONCLUSION

The atmospherically important OH radical was detected employing the state selective LIF technique from the photodissociation of PABA at 266 nm. The nascent OH radical was found to be vibrationally cold and its rotational state distribution showed a Boltzmann behavior with a rotational temperature of 1040±110 K, corresponding to the OH rotational energy of 8.78±0.84 kJ/mol. Preferential population of the $^2\Pi_{3/2}$ spin-orbit state of OH was observed implying participation of a nearby triplet state, and the population of the $\Pi(A')$ Λ-doublet state was predominant suggesting a nonplanar transition state geometry for the OH channel. Finally, according to the discussion of possible reaction mechanism for OH formation, we have proposed that the OH radical from the photodissociation of PABA at 266 nm was produced through the direct cleavage reaction of the C−OH bond with a considerable barrier in the exit channel.

V. ACKNOWLEDGMENTS

This work was supported by the National Natural Science Foundation of China (No.20721004 and No.20833008). Can-hua Zhou thanks to Dr. Ju-long Sun for assistance in the experiments.

[1] H. T. Kwon, S. K. Shin, S. K. Kim, H. L. Kim, and C. R. Park, J. Phys. Chem. A **105**, 6775 (2001).
[2] P. D. Naik, H. P. Upadhyaya, A. Kumar, A. V. Sapre, and J. P. Mittal, Chem. Phys. Lett. **340**, 116 (2001).
[3] A. Kumar, H. P. Upadhyaya, and P. D. Naik, J. Phys. Chem. A **108**, 6275 (2004).
[4] K. K. Pushpa, H. P. Upadhyaya, A. Kumar, P. D. Naik, and P. N. Bajaj, J. Chem. Phys. **120**, 6964 (2004).
[5] A. Kumar, H. P. Upadhyaya, P. D. Naik, D. K. Maity, and J. P. Mittal, J. Phys. Chem. A **106**, 11847 (2002).
[6] A. Kumar and P. D. Naik, Chem. Phys. Lett. **422**, 152 (2006).
[7] Q. Wei, J. L. Sun, X. F. Yue, H. M. Yin, and K. L. Han, Chem. Phys. Lett. **448**, 11 (2007).
[8] Q. Wei, J. L. Sun, X. F. Yue, S. B. Cheng, C. H. Zhou, H. M. Yin, and K. L. Han, J. Phys. Chem. A **112**, 4727 (2008).

DOI:10.1088/1674-0068/22/06/681-685

[9] C. H. Zhou, S. B. Cheng, J. L. Sun, H. M. Yin, K. L. Han, and G. Z. He, J. Phys. Chem. A **113**, 4923 (2009).
[10] D. H. Ehhalt, Science **279**, 1002 (1998).
[11] J. Matthews, A. Sinha, and J. S. Francisco, Proc. Natl. Acad. Sci. USA **12**, 7449 (2005).
[12] S. Xavier, S. MacDonald, J. Roth, M. Caunt, A. Akalu, D. Morais, M. T. Buckley, L. Liebes, S. C. Formenti, and P. C. Brooks, Int. J. Radiat. Oncol. Biol. Phys. **65**, 517 (2006).
[13] K. M. Hanson, E. Gratton, and C. J. Bardeen, Free Radical Biol. Med. **41**, 1205 (2006).
[14] G. Meijer, M. S. de Vries, H. E. Hunziker, and H. R. Wendt, J. Chem. Phys. **92**, 7625 (1990).
[15] Y. G. He, C. Y. Wu, and W. Kong, J. Phys. Chem. A **109**, 2809 (2005).
[16] Y. G. He, C. Y. Wu, and W. Kong, J. Chem. Phys. **121**, 3533 (2004).
[17] X. X. Zhang, J. L. Oscarson, R. M. Izatt, P. C. Schuck, and D. Li, J. Phys. Chem. B **104**, 8598 (2000).
[18] I. Compagnon, R. Antoine, and D. Rayane, J. Phys. Chem. A **107**, 3036 (2003).
[19] D. M. Mitchell, P. J. Morgan, and D. W. Pratt, J. Phys. Chem. A **112**, 12597 (2008).
[20] O. Rubio-Pons and Y. Luo, J. Chem. Phys. **121**, 157 (2004).
[21] A. F. Lago, J. Z. Davalos, and A. Naves de brito, Chem. Phys. Lett. **443**, 232 (2007).
[22] H. M. Yin, J. L. Sun, Y. M. Li, K. L. Han, and G. Z. He, J. Chem. Phys. **118**, 8248 (2003).
[23] X. F. Yue, J. L. Sun, Q. Wei, H. M. Yin, and K. L. Han, Chin. J. Chem. Phys. **20**, 401 (2007).
[24] C. H. Zhou, S. B. Cheng, J. L. Sun, H. M. Yin, K. L. Han, and G. Z. He, Chem. Phys. Lett. **466**, 27 (2008).
[25] K. P. Huber and G. Herzberg, *Molecular Spectra and Molecular Structure: Constants of Diatomic Molecules, Vol IV*, New York: Van Nostrand, (1979).
[26] J. Luque and D. R. Crosley, J. Chem. Phys. **109**, 439 (1998).
[27] I. Kovacs, *Rotational Structure in the Spectra of Diatomic Molecule*, London: Adam Hilger Ltd., (1969).
[28] R. Vasudev, R. N. Zare, and R. N. Dixon, J. Chem. Phys. **80**, 4863 (1984).
[29] K. L. Han and G. Z. He, J. Photochem. Photobiol. C **8**, 55 (2007).
[30] T. S. Chu, Y. Zhang, and K. L. Han, Inter. Rev. Phys. Chem. **10**, 2431 (2006).
[31] H. Zhang, R. S. Zhu, G. J. Wang, K. L. Han, and N. Q. Lou, J. Chem. Phys. **110**, 2922 (1999).
[32] M. H. Alexander, P. Andresen, R. Bacis, R. Bersohn, F. J. Comes, P. J. Dagdigian, R. N. Dixon, R. W. Field, G. W. Flynn, K. H. Gericke, E. R. Grant, B. J. Howard, J. R. Huber, D. S. King, J. L. Kinsey, K. Kleinermanns, K. Kuchitsu, A. C. Luntz, A. J. McCaffery, B. Pouilly, H. Reisler, S. Rosenwaks, E. W. Rothe, M. Shapiro, J. P. Simons, R. Vasudev, J. R. Wiesenfeld, C. Wittig, and R. N. Zare, J. Chem. Phys. **89**, 1749 (1988).

DOI:10.1088/1674-0068/22/06/681-685